



# RESEARCH MEMORANDUM

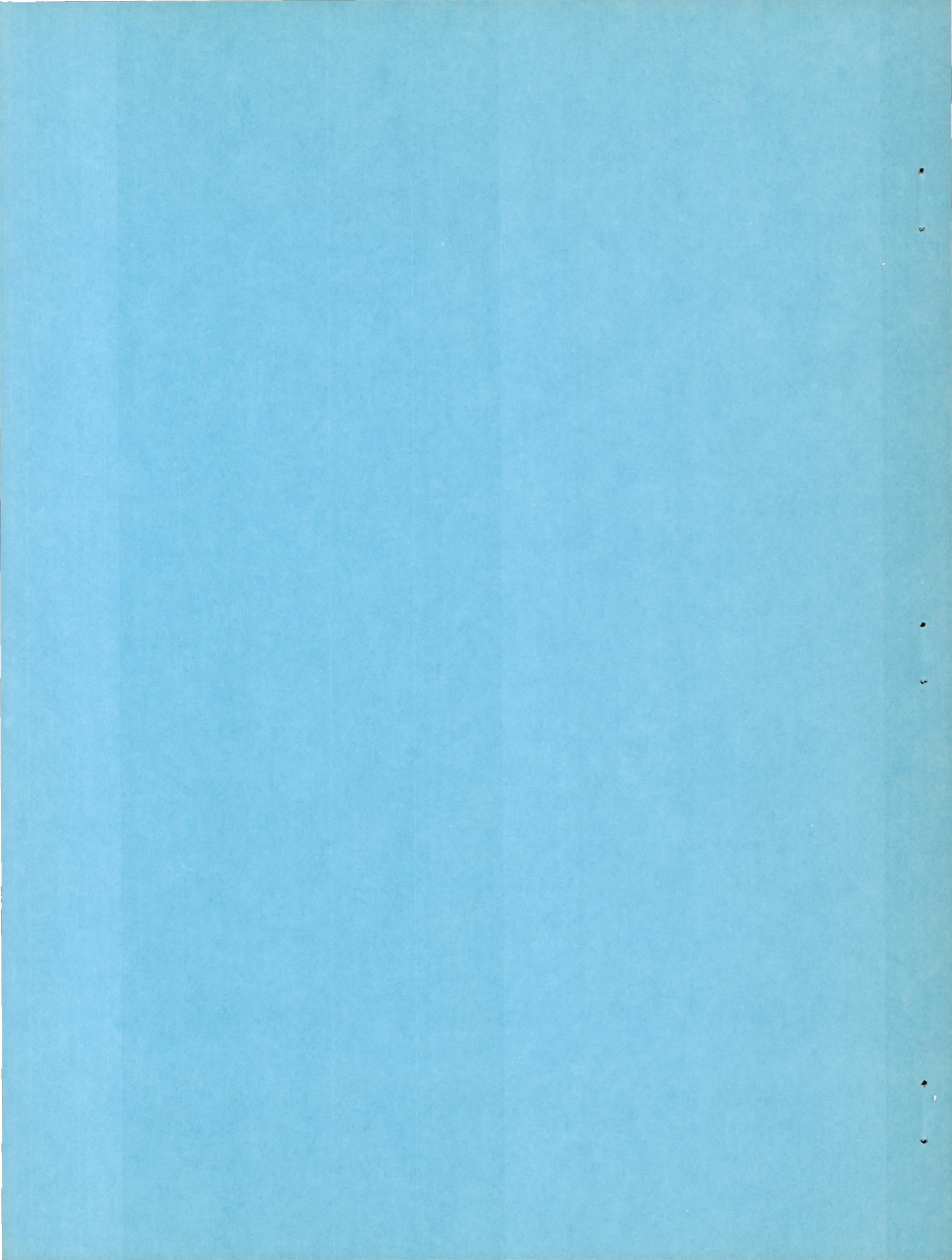
THEORETICAL INVESTIGATION OF THE DYNAMIC LATERAL  
STABILITY CHARACTERISTICS OF THE DOUGLAS  
X-3 RESEARCH AIRPLANE, STUDY 41-B

By Charles V. Bennett

Langley Aeronautical Laboratory  
Langley Air Force Base, Va.

NATIONAL ADVISORY COMMITTEE  
FOR AERONAUTICS

WASHINGTON  
April 27, 1950



## NATIONAL ADVISORY COMMITTEE FOR AERONAUTICS

## RESEARCH MEMORANDUM

## THEORETICAL INVESTIGATION OF THE DYNAMIC LATERAL

## STABILITY CHARACTERISTICS OF THE DOUGLAS

## X-3 RESEARCH AIRPLANE, STUDY 41-B

By Charles V. Bennett

## SUMMARY

Calculations have been made of the dynamic lateral stability characteristics of the mock-up configuration of the Douglas X-3 research airplane, designated by the Douglas Aircraft Co., Inc. as study 41-B. Because of a doubt as to the correct value of  $C_{np}$  for the airplane, duplicate results are presented for calculations made with the estimated values of  $C_{np}$  and with values based on experiment. The calculations indicate that for the mass and aerodynamic parameters used, the oscillation of the airplane would be stable for all conditions investigated but would not meet the Air Force damping requirement for the majority of the conditions. Less stability was calculated for all cases when the values of  $C_{np}$  based on experiment were used than when the estimated (more positive) values of  $C_{np}$  were used. The calculations indicate that the damping of the lateral oscillation could be improved by decreasing the wing incidence, by adding vertical-fin area forward of the center of gravity or by decreasing the dihedral, but no geometric arrangement was found that would make the airplane completely satisfactory from the standpoint of oscillation damping, ratio of roll to sideslip, and aileron required to hold a sideslip. The calculations indicate that a great improvement in oscillation damping could be obtained for all conditions by use of an autopilot which artificially produced  $C_{np}$  or  $C_{nr}$  and for the  $M = 0.75$  condition with an autopilot which produced  $-C_{lp}$ .

## INTRODUCTION

A study of the theoretical dynamic lateral stability characteristics of the Douglas X-3 research airplane (study 39-C) was reported in reference 1. The final mock-up configuration (study 41-B), shown in figure 1,

differs appreciably from that used in reference 1. Some of the mass and geometric differences of the two studies are shown on table I. Because of these revisions, additional calculations have been made of the dynamic lateral stability characteristics of the more recent mock-up configuration. These calculations were made for Mach numbers of 0.75, 1.2, and 2.0.

All calculations were based on the mass and aerodynamic parameters supplied by the Douglas Aircraft Co., Inc. with the exception of  $C_{n_p}$ , the yawing-moment coefficient due to rolling. A recent study has shown that there is usually a marked disagreement between the measured and estimated values of  $C_{n_p}$  contributed by the vertical tail of the airplane. The disagreement is apparently present at all angles of attack and is such that the measured values are always either less positive or more negative than the estimated values. The disagreement is apparently caused by the fact that present estimation procedures do not take into account the sidewash over the vertical tail that is produced by the rolling wing. In order to check this point for the Douglas X-3, experimental values of  $C_{n_p}$  for tail off and tail on were obtained at low angles of attack for the free-flight-tunnel model of the airplane on the rotary balance in the Langley 20-foot free-spinning tunnel and were compared with estimated values. The results showed that the measured tail contribution to  $C_{n_p}$  was appreciably more negative than the estimated value. As a result, all calculations of the present study have been made for both the estimated values of  $C_{n_p}$  and values of  $C_{n_p}$  based on experiment.

An undamped residual (snaking) oscillation of small amplitude has existed on several airplanes. In some cases this oscillation was caused by rudder motion or fuel sloshing. It is believed that other cases were caused by nonlinearity in the aerodynamic characteristics. These factors have not been considered in this analysis.

#### SYMBOLS AND COEFFICIENTS

S	wing area, square feet
V	airspeed, feet per second
b	wing span, feet
$\rho$	air density, slugs per cubic foot
q	dynamic pressure, pounds per square foot $\left(\frac{1}{2}\rho V^2\right)$

W	weight, pounds
g	acceleration of gravity, feet per second per second
m	mass, slugs ( $W/g$ )
$\mu_b$	relative density factor based on wing span ( $m/\rho S b$ )
$\epsilon$	angle between reference axis and principal axis; positive when reference axis is above principal axis at nose, degrees
$\eta$	angle of attack of principal longitudinal axis of airplane; positive when principal axis is above flight path at nose, degrees
$\gamma$	angle of flight to horizontal axis; positive in a climb, degrees
$\beta$	angle of sideslip, degrees; except in equations of motion, per radian
$\delta_r$	rudder deflection, degrees
$\phi$	angle of bank, degrees; except in equations of motion, per radian
$\psi$	angle of azimuth, degrees; except in equations of motion, per radian
$\Gamma$	angle of geometric dihedral, degrees
i	incidence, degrees
$I_{X_0}$	moment of inertia about principal longitudinal axis, pound-inches <sup>2</sup>
$I_{Z_0}$	moment of inertia about principal vertical axis, pound-inches <sup>2</sup>
$I_{Y_0}$	moment of inertia about principal pitching axis, pound-inches <sup>2</sup>
$k_{X_0}$	radius of gyration about principal longitudinal axis, feet
$k_{Z_0}$	radius of gyration about principal vertical axis, feet
$K_{X_0}$	nondimensional radius of gyration about principal longitudinal axis ( $k_{X_0}/b$ )

$K_{Z_0}$	nondimensional radius of gyration about principal vertical axis $(k_{Z_0}/b)$
$K_X$	nondimensional radius of gyration about longitudinal stability axis $\left(\sqrt{K_{X_0}^2 \cos^2 \eta + K_{Z_0}^2 \sin^2 \eta}\right)$
$K_Z$	nondimensional radius of gyration about vertical stability axis $\left(\sqrt{K_{Z_0}^2 \cos^2 \eta + K_{X_0}^2 \sin^2 \eta}\right)$
$K_{XZ}$	nondimensional product-of-inertia parameter $\left((K_{Z_0}^2 - K_{X_0}^2) \cos \eta \sin \eta\right)$
$C_L$	lift coefficient (Lift/qS)
$C_n$	yawing-moment coefficient $\left(\frac{\text{Yawning moment}}{qSb}\right)$
$C_l$	rolling-moment coefficient $\left(\frac{\text{Rolling moment}}{qSb}\right)$
$C_Y$	lateral-force coefficient $\left(\frac{\text{Lateral force}}{qS}\right)$
$C_{Y_\beta}$	rate of change of lateral-force coefficient with angle of sideslip, per radian $\left(\frac{\partial C_Y}{\partial \beta}\right)$
$C_{n_\beta}$	rate of change of yawing-moment coefficient with angle of sideslip, per radian $\left(\frac{\partial C_n}{\partial \beta}\right)$
$C_{l_\beta}$	rate of change of rolling-moment coefficient with angle of sideslip, per radian $\left(\frac{\partial C_l}{\partial \beta}\right)$
$C_{Y_p}$	rate of change of lateral-force coefficient with rolling-angular-velocity factor, per radian $\left(\frac{\partial C_Y}{\partial \frac{pb}{2V}}\right)$
$C_{l_p}$	rate of change of rolling-moment coefficient with rolling-angular-velocity factor, per radian $\left(\frac{\partial C_l}{\partial \frac{pb}{2V}}\right)$

$C_{n_p}$  rate of change of yawing-moment coefficient with rolling-angular-velocity factor, per radian  $\left( \frac{\partial C_n}{\partial \dot{\theta}^2 V} \right)$

$C_{l_r}$  rate of change of rolling-moment coefficient with yawing-angular-velocity factor, per radian  $\left( \frac{\partial C_l}{\partial \dot{\theta}^2 V} \right)$

$C_{n_r}$  rate of change of yawing-moment coefficient with yawing-angular-velocity factor, per radian  $\left( \frac{\partial C_n}{\partial \dot{\theta}^2 V} \right)$

$l$  tail length (distance from center of gravity to rudder hinge line), feet

$\bar{z}$  height of center of pressure of vertical tail above fuselage axis, feet

$p$  rolling-angular velocity, radians per second

$r$  yawing-angular velocity, radians per second

$P$  period of oscillation, seconds

$T_{1/2}$  time for oscillation to damp to one-half amplitude

$C_{1/2}$  cycles for oscillation to damp to one-half amplitude

$M$  Mach number

$h$  altitude, feet

Subscripts:

$t$  tail

$w$  wing

## CALCULATIONS

The equations of reference 2 were utilized to determine the period and damping of the oscillation for the six basic level-flight conditions as follows:

Condition	Mach number	Altitude (ft)	$C_L$
I	0.75	0	0.15
II	.75	35,000	.65
III	1.2	35,000	.25
IV	1.2	50,000	.51
V	2.0	35,000	.09
VI	2.0	50,000	.18

The mass and aerodynamic parameters used in the calculations are shown in table II. Some independent calculations of the aerodynamic parameters were made for comparison with the values furnished by Douglas Aircraft Co., Inc. Where direct comparisons were possible, fairly good agreement was found between the two sets of values with the exception of the yawing due to rolling parameter  $C_{n_p}$ . A complete check could not be made, however, because of the uncertainty as to the effects of changes in the tail-boom design on the static-stability derivatives of the airplane. Another questionable point was the large variation with altitude shown for some of the stability derivatives estimated by Douglas Aircraft Co., Inc. Some additional calculations were therefore made to determine the effect of possible errors made in estimating the tail-effectiveness factor  $C_{Y_{\beta_t}}$  and the damping-in-roll parameter  $C_{l_p}$ . The tail-effectiveness factor  $C_{Y_{\beta_t}}$  was increased and decreased 50 percent and the damping-in-roll factor  $C_{l_p}$  was increased and decreased 25 percent. The derivative  $C_{Y_{\beta_t}}$  was chosen as one of the variables since, for this airplane, it contributes over 70 percent of the total value of the derivatives  $C_{n_p}$ ,  $C_{n_r}$ ,  $C_{n_p}$ , and  $C_{l_r}$ , and also contributes fairly large amounts to  $C_{l_p}$  and  $C_{Y_p}$ . The derivative  $C_{l_p}$  is an important derivative that was varied because it is produced mainly by the wing and is not affected much by changes in  $C_{Y_{\beta_t}}$ .

Calculations were also made to determine the effect on the period and time to damp of some geometric changes to the airplane which included a decrease in the wing incidence, a decrease in the geometric dihedral, and a vertical-tail modification. The effect of an autopilot (with zero lag) which changed  $C_{n_r}$ ,  $C_{n_p}$ , and  $C_{l_p}$  was also studied.

All calculations were made with the values of  $C_{n_p}$  obtained from the Douglas Aircraft Co., Inc. and also with the values of  $C_{n_p}$  which were estimated at the Langley free-flight tunnel. The values of  $C_{n_p}$  which were estimated at the Langley free-flight tunnel were based on unpublished experimental values of  $C_{n_p}$  which were obtained for the free-flight-tunnel model of the X-3 (reference 1). These experimental data indicated that the values of  $C_{n_p}$  estimated by the method of reference 3 for this model were too high by an increment of about 0.125 over the angle-of-attack range under consideration. The value of  $C_{Y\beta_t}$  for the free-flight model (-0.30) was appreciably different from the estimated values of  $C_{Y\beta_t}$  for the airplane for the six flight conditions because of the differences in Mach number, because of the low scale of the free-flight-tunnel tests, and because of the differences in tail size and tail location. Since  $C_{n_p}$  is directly related to  $C_{Y\beta_t}$ , the incremental value of  $C_{n_p}$  (0.125) was multiplied by the ratio  $\frac{(C_{Y\beta_t})_{\text{Airplane}}}{(C_{Y\beta_t})_{\text{Model}}}$  to obtain the value to be subtracted from the estimated values of  $C_{n_p}$  for the airplane, as illustrated by the following formula:

$$C_{n_p}(\text{free-flight estimate}) = C_{n_p}(\text{estimated from ref. 3}) - \\ \left[ 0.125 \frac{(C_{Y\beta_t})_{\text{Airplane}}}{-0.30} \right]$$

Although the values of  $C_{n_p}$  based on experiment were used, it should be pointed out that they are probably not quantitatively correct because they are based on low-scale data. The uncertainty as to the correct values of  $C_{n_p}$  for the high-speed conditions, which are included herein, make it necessary to consider the results as being only of a qualitative nature.

The tail contribution to damping in roll  $C_{l_{pt}}$  should also be expected to be different because of the effect of the rolling wing on the tail effectiveness, but this effect should be small and has therefore been neglected.

## RESULTS AND DISCUSSION

### Spiral Mode

The spiral mode is stable for all conditions investigated, as shown in table II, and, therefore, easily satisfies the Air Force requirement for spiral stability.

### Oscillatory Stability of the Basic Airplane

The results of the calculated oscillatory stability characteristics are shown in figures 2 to 4 and are also summarized in table II. The results show that with either value of  $C_{n_p}$  the damping for the majority of the conditions would not be great enough to meet the Air Force damping requirement but indicate that the airplane would be stable for all conditions. In all cases, the calculations indicated less stability when the values of  $C_{n_p}$  based on experiment were used than when the values estimated by the Douglas Aircraft Co., Inc. were used. The data also indicate that an increase in tail effectiveness decreased both the period and the time in seconds to damp to one-half amplitude so that the damping in terms of cycles (or the distance from the criterion boundary) did not change nearly so much as the damping in terms of seconds.

The effect on the period and damping of the lateral oscillation of increasing or decreasing  $C_{l_p}$  by 25 percent for Mach numbers of 0.75, 1.2, and 2.0 at 35,000 feet is shown in figure 5. These data indicate that for either value of  $C_{n_p}$ , an increase in  $C_{l_p}$  for the  $M = 0.75$  condition resulted in an increase in stability; whereas an increase in  $C_{l_p}$  for the  $M = 2.0$  condition slightly decreased the damping. There was virtually no change in the damping for the  $M = 1.2$  condition when  $C_{l_p}$  was increased or decreased 25 percent. The data also indicate that the damping was appreciably decreased for all conditions when the values of  $C_{n_p}$  based on experiment were used instead of those estimated by the Douglas Aircraft Co., Inc.

It appears from these results that small errors in the estimation of  $C_{l_p}$  or of the tail-effectiveness factor  $C_{Y\beta_t}$  will not greatly

affect the accuracy of predicting the dynamic lateral stability of this airplane in the terms of cycles to damp to one-half amplitude and hence in terms of the distance from the criterion boundary. It does appear, however, that an accurate estimation of  $C_{np}$  is necessary to predict the lateral stability with reasonable accuracy. It is also necessary to have very accurate knowledge of the inclination of the principal longitudinal axis of inertia of the airplane as shown in reference 1 and in calculations made by the Douglas Aircraft Co., Inc.

#### Oscillatory Stability of Modified Airplane

The results of calculations made to determine the effect of several possible geometric modifications to the airplane are shown in figures 6 and 7 and are summarized in table III. Computations of the period and time to damp to one-half amplitude for only the  $M = 2.0$  condition at 35,000 feet were made to determine the effect of these changes. The value of  $C_{np}$  calculated by the Douglas Aircraft Co., Inc. was used for the points of figure 6(a) and the value of  $C_{np}$  based on experiment was used for the points of figure 6(b). The (A) points of this figure show that the period and time to damp for the original  $M = 2.0$  condition at 35,000-foot altitude would not meet the Air Force damping requirement for either value of  $C_{np}$ .

The effect of a  $5^\circ$  reduction in dihedral is shown by the (B) points of figure 6. The  $5^\circ$  reduction in dihedral was investigated both as a possible means of increasing the damping and as a means of reducing the ratio of oscillatory amplitude of roll to sideslip which, for this condition was relatively high (about 5) because of the high ratio of yawing inertia to rolling inertia. Figure 6(a) shows that when the value of  $C_{np}$  estimated by the Douglas Aircraft Co., Inc. was used, the damping was decreased when the dihedral was decreased but when the value of  $C_{np}$  based on experiment was used the damping was increased when the dihedral was decreased. The opposite effect of decreasing the dihedral for the two values of  $C_{np}$  is partly caused by the fact that the term  $(C_{np} - 2C_LKZ^2)$  was positive for the value of  $C_{np}$  estimated by the Douglas Aircraft Co., Inc. and negative for the value of  $C_{np}$  which was based on experiment. A more complete discussion of this effect is given in reference 4. Figure 7 shows that the ratio of roll to sideslip was reduced from approximately 5 to 2.5 when the dihedral was reduced. The reduction in the ratio of roll to sideslip was approximately the same regardless of the value of  $C_{np}$  used. Although it is not known if the large ratio of roll to sideslip for the original dihedral condition would be considered undesirable, some investigators have thought that the ratio should not be more than 2.5. The ratio of roll to sideslip which was obtained from figure 7 by measurement of the amplitudes of the bank and

sideslip angles for the two dihedral configurations can also be approximated by the following formula:

$$\left| \frac{\phi}{\beta} \right| = \frac{l_v}{n_v} \frac{1}{\sqrt{1 + \frac{l_p^2}{\mu_b n_v}}}$$

where

$$l_v = \frac{C_l \beta}{2K_X^2}$$

$$n_v = \frac{C_n \beta}{2K_Z^2}$$

$$l_p = \frac{C_l p}{4K_X^2}$$

The data of figure 7 indicate also that with either value of  $C_{n_p}$  the airplane would initially bank in the wrong direction after a rudder kick for both dihedral conditions. This initial adverse rolling due to a rudder kick is not unusual and is caused by the high location of the rudder with respect to the center of gravity. With the original dihedral, the airplane reversed this direction of bank because of the dihedral effect; whereas in the reduced dihedral condition the airplane remained banked in the wrong direction after a rudder kick because of insufficient dihedral effect. Further analysis indicates that, for the reduced dihedral condition, aileron control opposite to that normally required would be necessary to hold a steady sideslip and the airplane would not meet the Air Force flying-qualities requirements in this respect. It is shown in the appendix that for the  $M = 2.0$  condition,  $C_l \beta$  must be greater than  $-\frac{1}{4} C_{n_p}$  to meet this requirement. The ratio of  $C_l \beta$  to  $-C_{n_p}$  for the reduced dihedral condition (table III) is less than 1/4.

The (C) points of figure 6 indicate that a reduction of  $1^\circ$  in wing incidence increased the damping of the oscillation and that for the calculation made with the Douglas estimated value of  $C_{n_p}$  the increase in damping was great enough to meet the Air Force damping requirement. When the  $C_{n_p}$  based on experiment was used, however, the increase in damping caused by  $1^\circ$  incidence decrease was not nearly great enough to meet this damping requirement. When  $C_{n_p}$  was reduced by 50 percent in

combination with the decreased wing incidence (points (D)), the damping was further improved for the calculation made with the Douglas estimated value of  $C_{n_p}$  but was not changed when the value of  $C_{n_p}$  based on experiment was used. The (D) points also show that the period was increased about 1/2 second by decreasing  $C_{n_\beta}$  by 50 percent for either  $C_{n_p}$ . The ratio of roll to sideslip was not improved by decreasing either  $C_{n_\beta}$  or the wing incidence. In fact, the condition shown by the (D) points, resulted in a larger ratio of roll to sideslip because of the reduced  $C_{n_\beta}$ .

The (E) points of figure 6 represent the airplane with  $1^\circ$  negative wing incidence, with  $C_{n_\beta}$  reduced 50 percent, and with  $-5^\circ$  dihedral.

The only difference in the airplane configuration between points (D) and (E) is the  $5^\circ$  decrease in dihedral and therefore a similar effect on the damping is shown as was shown and discussed for points (A) and (B). The ratio of roll to sideslip was not decreased appreciably from the original value of 5 because the decrease in dihedral  $-C_{l_\beta}$  was about balanced by the decrease in  $C_{n_\beta}$ . Even with this reduced dihedral the aileron to hold sideslip was in the desired direction because  $C_{l_\beta}$  was still greater than  $-\frac{1}{4}C_{n_\beta}$ .

The (F) points of figure 6 represent the airplane with  $1^\circ$  negative incidence, with the dihedral approximately  $-7^\circ$ , and with a vertical fin added on the nose of the airplane in such a manner that  $C_{n_\beta}$  was reduced 50 percent and  $C_{n_r}$  was increased 75 percent. For this configuration the ratio of roll to sideslip was decreased to 2.5 and the damping was made satisfactory for both values of  $C_{n_p}$ . As in the case of the (B) points, however, the aileron control required in a steady sideslip would be reversed.

Although these calculations for the airplane with the geometric revisions were made only for the  $M = 2.0$  condition which was considered critical, it is believed that similar trends would be obtained for the  $M = 0.75$  and  $M = 1.2$  conditions with the exception that the opposite effect of  $C_{l_p}$  on the damping would be expected as has been discussed previously.

Autopilot additions. - The effect of varying the rotary-stability derivatives  $C_{n_p}$ ,  $C_{n_r}$ , and  $C_{l_p}$  to simulate the addition of a rate gyro autopilot with zero time lag and installed in the airplane so as to vary only one derivative at a time was investigated for Mach numbers of 0.75, 1.2, and 2.0 at 35,000-foot altitude and the results are shown in figures 8 to 10. The derivative  $C_{n_p}$  was varied from -0.10 to 1.0;

$C_{l_p}$  from 0 to -3.0; and  $C_{n_r}$  from 0 to -10.0. The mass and aerodynamic parameters used for these calculations are those shown in table II except that  $C_{n_p}$  values of -0.105, 0.084, and 0.047 were used for the Mach numbers of 0.75, 1.2, and 2.0, respectively. The different values of  $C_{n_p}$  were used for the autopilot calculations because at the time these calculations were made a different method was being used to correct the experimental  $C_{n_p}$  data of the model to high-speed full-scale values.

Since it is not known what the correct values of  $C_{n_p}$  for the airplane are and since the effects of autopilot lag have been neglected, these results should be considered as of a qualitative nature only. In some cases the curves representing the damping of the spiral and rolling modes (aperiodic modes) are not shown for the complete range of variables because in these cases the aperiodic modes combined to form a very long-period oscillation and then reappeared as a very slightly unstable aperiodic mode.

The calculated data of figures 8 and 9 indicate that increasing  $C_{n_p}$  in the positive direction or  $C_{n_r}$  in the negative direction increased the damping of the oscillation, had virtually no effect on the period, increased the damping of the spiral mode, and only slightly decreased the damping of the rolling mode for all Mach numbers investigated. The data of figure 10 show that increasing the damping-in-roll parameter  $-C_{l_p}$  increased the damping for the  $M = 0.75$  condition up to a value of  $C_{l_p} = -1.2$  and that a further increase in  $-C_{l_p}$  slightly reduced the damping. No effect on the damping is shown for the  $M = 1.2$  condition. A slight destabilizing effect of increasing the damping in roll is shown for the  $M = 2.0$  condition up to values of  $C_{l_p} = -0.6$  and a further increase in the damping in roll for this condition was slightly stabilizing. Increasing  $-C_{l_p}$  slightly increased the period for only the  $M = 0.75$  condition. The damping of the spiral mode was decreased by increasing  $-C_{l_p}$  and the damping of the rolling mode was increased by increasing  $-C_{l_p}$ .

The oscillation damping data of figures 8 to 10 have been summarized in figure 11 to show the relative merits of the three zero-lag autopilots considered. In this figure the incremental values of each derivative (produced by the autopilot) is plotted as the abscissa. It appears from these results that on the basis of the required change in the magnitude of the derivative to meet the Air Force damping requirement, an autopilot which artificially produced  $C_{n_p}$  would be most effective in improving the damping of the lateral oscillation for the three conditions investigated. This comparison involving only the magnitude of the changes in the derivatives is not believed to be completely valid, however, because of the limitations to the control moment available for the

autopilot; that is, for the higher values of the derivatives the maximum possible control-surface deflection would be reached before the maximum rolling or yawing velocities would be reached and a nonlinear condition would therefore result. Since the ratio of rolling velocity to yawing velocity is rather large for this airplane, it should be expected that this nonlinear condition would occur for a smaller value of  $C_{n_p}$  than  $C_{n_r}$ . Since this comparison is for autopilots with zero time lag it is likely that it may not be completely valid for autopilots with appreciable time lag. Further study is required to establish more definitely the relative merits of the different type autopilots.

#### CONCLUSIONS

The following conclusions are drawn from the results of the theoretical study of the dynamic lateral stability characteristics of the X-3 research airplane, study 41-B.

1. With the mass and aerodynamic parameters used in this investigation the oscillation of the airplane would be stable for all conditions but would not meet the Air Force damping requirement for the majority of the conditions investigated. Less stability was calculated for all cases when the values of  $C_{n_p}$  based on experiment were used than when the estimated (more positive) values of  $C_{n_p}$  were used.
2. The damping of the lateral oscillation of the airplane can be improved by decreasing the wing incidence, by adding vertical-fin area forward of the center of gravity, or by decreasing the dihedral, but no geometric arrangement was found that would make the airplane completely satisfactory from the standpoint of oscillation damping, ratio of roll to sideslip, and aileron required to hold a sideslip.

3. Great improvement can be obtained in oscillation damping for all conditions by use of an autopilot which artificially produced  $C_{n_p}$  or  $C_{n_r}$  and for the  $M = 0.75$  condition with an autopilot which produced  $-C_{l_p}$ .

Langley Aeronautical Laboratory  
National Advisory Committee for Aeronautics  
Langley Air Force Base, Va.

## APPENDIX

## AILERON DEFLECTION IN A STEADY SIDESLIP

The Air Force flying-qualities requirements state that in a steady sideslip, up-aileron deflection on the forward wing shall be required. This means that right-aileron deflection or right rolling moment is required to hold a right sideslip. It is necessary, therefore, that in a right sideslip the sum of the rolling moments produced by sideslip and by the rudder should be negative, or

$$(C_l \beta) + (C_l \delta_r \delta_r) < 0 \quad (1)$$

For a right sideslip, the term  $C_l \beta$  is usually negative and the term  $C_l \delta_r \delta_r$  is usually positive, so the requirement might be restated as

$$C_l \beta > - (C_l \delta_r \delta_r) \quad (2)$$

If the aileron yawing moments are neglected, in a steady sideslip

$$\delta_r = \frac{C_{n\beta} \beta}{C_{n\delta_r}} \quad (3)$$

Substituting equation (3) in equation (2) and dividing by  $\beta$  gives

$$C_l \beta > - \left( \frac{C_l \delta_r}{C_{n\delta_r}} C_{n\beta} \right) \quad (4)$$

Assuming that the rudder moments are proportional to the rudder-moment arms

$$\frac{C_l \delta_r}{C_{n\delta_r}} = \frac{\bar{z} - l \sin \alpha}{l \cos \alpha} \quad (5)$$

For the X-3 airplane at  $M = 2$  this ratio is approximately  $-\frac{1}{4}$ . Substituting this value in equation (4) gives

$$C_{l\beta} > -\frac{1}{4} C_{n\beta} \quad (6)$$

or,  $C_{l\beta}$  must be greater than  $-\frac{1}{4} C_{n\beta}$  to meet the Air Force requirement for aileron deflection in a steady sideslip.

## REFERENCES

1. Bennett, Charles V.: Theoretical Investigation of the Dynamic Lateral Stability Characteristics of Douglas Design No. 39C, an Early Version of the X-3 Research Airplane. NACA RM L8L31, 1949.
2. Sternfield, Leonard: Some Considerations of the Lateral Stability of High-Speed Aircraft. NACA TN 1282, 1947.
3. Bamber, Millard J.: Effect of Some Present-Day Airplane Design Trends on Requirements for Lateral Stability. NACA TN 814, 1941.
4. Sternfield, Leonard, and Gates, Ordway B., Jr.: A Simplified Method for the Determination and Analysis of the Neutral-Lateral Oscillatory-Stability Boundary. NACA Rep. 943, 1949.

TABLE I

## FUNDAMENTAL DIFFERENCES BETWEEN STUDY 39-C and 41-B

[Other geometric changes include the fuselage shape, the tail boom cross section, and the vertical tail size and location]

Factor	Study 39-C (reference 1)	Study 41-B Mock-up airplane
Wing incidence, deg . . . . .	1	0
b, ft . . . . .	21.92	22.69
W, lb . . . . .	14,153	20,800
I <sub>XO</sub> . . . . .	<sup>a</sup> 17,258,400	17,694,000
I <sub>ZO</sub> . . . . .	<sup>a</sup> 297,737,760	298,424,000
I <sub>YO</sub> . . . . .	<sup>a</sup> 287,598,400	285,187,000
ε, deg . . . . .	2	3

<sup>a</sup>These inertia values were approximately two times too large for the weight of 14,153 pounds.



TABLE II

FACTORS USED IN CALCULATIONS OF PERIOD AND TIME TO DAMP

M	0.75						1.2						2.0					
$\frac{h}{\mu_b}$	0 71.9						35,000 232.6						35,000 474.5					
$\left(\frac{k_{X_0}}{b}\right)^2$	.01148						.01148						.01148					
$\left(\frac{k_{Z_0}}{b}\right)^2$	.1935						.1935						.1935					
$\eta$ , deg	-.9						6						.15					
$K_X^2$	.01152						.01348						.01148					
$K_Z^2$	.1934						.1917						.1935					
$K_{ZX}$	-.00286						.01891						.00048					
$C_L$	.15						.64						.249					
$\frac{m}{\rho SV}$	1.95						7.25						4.52					
													9.24					
													2.71					
													5.54					
$\frac{C_{Y\beta_t}}{C_{Y\beta_t} \text{ (Douglas)}}$	0.5	1.0	1.5	0.5	1.0	1.5	0.5	1.0	1.5	0.5	1.0	1.5	0.5	1.0	1.5	0.5	1.0	1.5
$C_{Y\beta_t \text{ tail}}$	-.21	-.42	-.63	-.23	-.45	-.68	-.37	-.75	-.12	-.39	-.78	-.17	-.18	-.36	-.54	-.19	-.38	-.57
$C_{l_p}$	-.327	-.343	-.359	-.289	-.290	-.295	-.415	-.440	-.462	-.399	-.410	-.421	-.282	-.295	-.310	-.276	-.285	-.294
$C_{Y\beta}$	-.536	-.745	-.956	-.549	-.775	-.1001	-.699	-.075	-.451	-.710	-.110	-.490	-.502	-.690	-.867	-.513	-.710	-.898
$C_{l_r}$	.123	.205	.287	.202	.235	.269	.178	.310	.443	.159	.250	.351	.088	.160	.232	.087	.145	.207
Estimated by Douglas	.081	.164	.245	.021	.055	.090	.207	.340	.472	.219	.310	.401	.103	.175	.247	.115	.175	.235
Based on experiment	-.0065	-.011	-.0175	-.0727	-.1325	-.1912	.0508	.0275	.0033	.057	-.015	-.077	.028	.025	.022	.0358	.0166	-.0026
$C_{n_r}$	-.657	-1.050	-1.410	-.690	-1.090	-1.500	-1.050	-1.820	-2.590	-1.090	-1.900	-2.710	-.640	-1.020	-1.360	-.670	-1.080	-1.450
$C_{n\beta}$	.0082	.2979	.5077	.101	.327	.553	.287	.659	.1039	.309	.699	.1089	.0863	.2691	.4513	.105	.292	.490
$C_{l\beta}$	-.082	-.120	-.163	-.118	-.135	-.152	-.087	-.154	-.219	-.066	-.112	-.157	-.059	-.094	-.130	-.059	-.089	-.119
Oscillatory mode ( $C_{n_p}$ estimated by Douglas)																		
Period	3.214	1.756	1.347	3.449	2.453	1.987	2.187	1.442	1.149	2.686	1.812	1.459	2.599	1.414	1.083	2.854	1.754	1.365
$T_{1/2}$	4.017	1.577	1.021	2.651	2.421	2.020	2.711	1.543	1.086	3.295	2.329	1.771	3.827	1.834	1.297	3.049	2.483	2.005
$C_{1/2}$	1.25	0.90	0.76	0.77	0.99	1.02	1.24	1.07	0.95	1.23	1.29	1.21	1.47	1.30	1.20	1.07	1.41	1.48
Spiral mode ( $C_{n_p}$ estimated by Douglas)																		
$T_{1/2}$	11.172	25.090	32.037	13.593	30.217	38.603	67.671	81.932	91.734	135.683	188.454	256.420	27.955	51.485	64.179	35.795	57.340	73.144
Rolling mode ( $C_{n_p}$ estimated by Douglas)																		
$T_{1/2}$	0.183	0.184	0.185	1.295	1.093	1.048	0.372	0.370	0.372	0.905	0.882	0.874	0.307	0.317	0.319	0.830	0.771	0.754
Oscillatory mode ( $C_{n_p}$ based on experiment)																		
Period	2.92	1.65	1.27	3.41	2.41	1.97	2.15	1.42	1.13	2.67	1.80	1.45	2.47	1.39	1.07	2.82	1.74	1.36
$T_{1/2}$	8.60	2.73	1.77	3.55	3.44	2.97	4.00	2.33	1.65	4.09	3.05	2.37	12.09	3.60	2.32	4.41	3.63	2.95
$C_{1/2}$	2.94	1.65	1.39	1.04	1.43	1.51	1.86	1.64	1.46	1.53	1.69	1.63	4.89	2.59	2.18	1.56	2.09	2.17
Spiral mode ( $C_{n_p}$ based on experiment)																		
$T_{1/2}$	14.235	30.653	41.768	16.682	33.438	47.330	76.776	99.512	117.875	149.505	209.937	298.954	34.004	63.224	81.737	42.175	68.095	89.609
Rolling mode ( $C_{n_p}$ based on experiment)																		
$T_{1/2}$	0.173	0.167	0.159	1.069	0.924	0.865	0.342	0.320	0.303	0.840	0.787	0.751	0.275	0.270	0.260	0.714	0.652	0.618

$$C_{Y_p} = C_{Y_r} = \tan \gamma = 0$$

Tail contributions to the aerodynamic parameters (reference 3):

$$C_{l_{pt}} = 2\left(\frac{z}{b} - \frac{l}{b} \sin \alpha\right)^2 C_{Y_{\beta_t}}$$

$$C_{n_{\beta_t}} = -\frac{l}{b} C_{Y_{\beta_t}}$$

$$C_{n_{pt}} = C_{l_{rt}} \approx -2\frac{l}{b}\left(\frac{z}{b} - \frac{l}{b} \sin \alpha\right) C_{Y_{\beta_t}}$$

$$C_{l_{\beta_t}} = \left(\frac{z}{b} - \frac{l}{b} \sin \alpha\right) C_{Y_{\beta_t}}$$

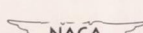


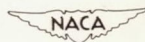
TABLE III  
RESULTS OF GEOMETRIC MODIFICATIONS TO AIRPLANE  
[ $M = 2.0$ ;  $h = 35,000$  feet]

Condition	$\Gamma$	$i_w$	$C_{l\beta}$	$C_{n\beta}$	$C_{n_r}$	$C_{n_p}$	Damping (a)	$ \frac{\phi}{\beta} $ (b)	Aileron to hold sideslip (c)
A	0	0	-0.094	0.269	-1.02	0.175 .025	U U	U U	S S
B	-5	0	-.051	.269	-1.02	.175 .025	U U	S S	U U
C	0	-1	-.094	.269	-1.02	.175 .025	S U	U U	S S
D	0	-1	-.094	.135	-1.02	.175 .025	S U	U U	S S
E	-5	-1	-.051	.135	-1.02	.175 .025	S U	U U	S S
F	-7	-1	-.024	.135	-1.79	.175 .025	S S	S S	U U

<sup>a</sup>The damping is considered satisfactory (S) when the Air Force damping requirement is satisfied and unsatisfactory (U) when the requirement is not satisfied.

<sup>b</sup>The values of  $|\frac{\phi}{\beta}|$  were 2.5 or less for the cases marked satisfactory (S) and 5 or more for the cases marked unsatisfactory (U).

<sup>c</sup>The aileron to hold a sideslip is considered satisfactory (S) if up aileron on the forward wing is required and unsatisfactory (U) if down aileron on the forward wing is required.



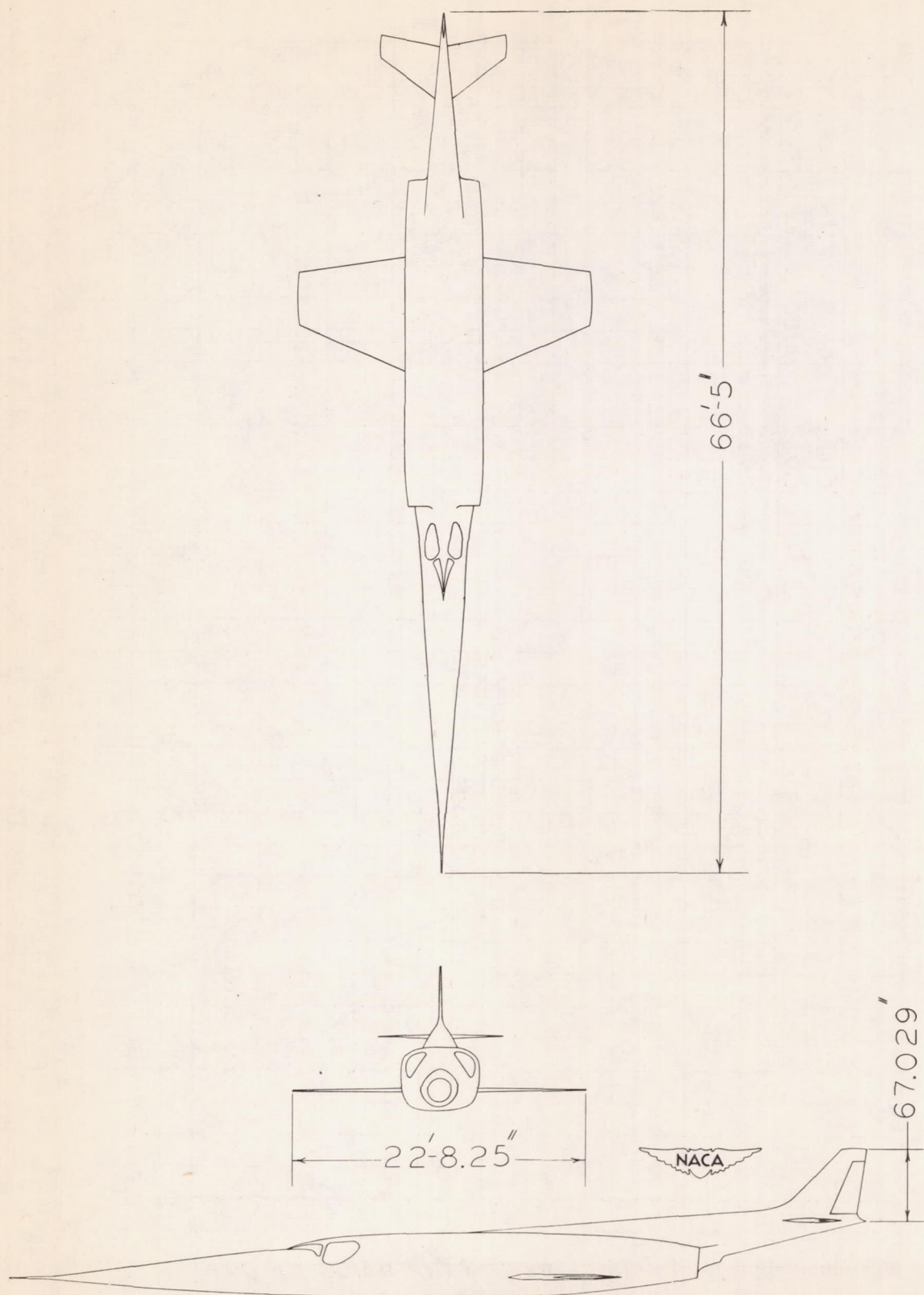


Figure 1.- Three-view sketch of Douglas X-3 research airplane, study 41-B.

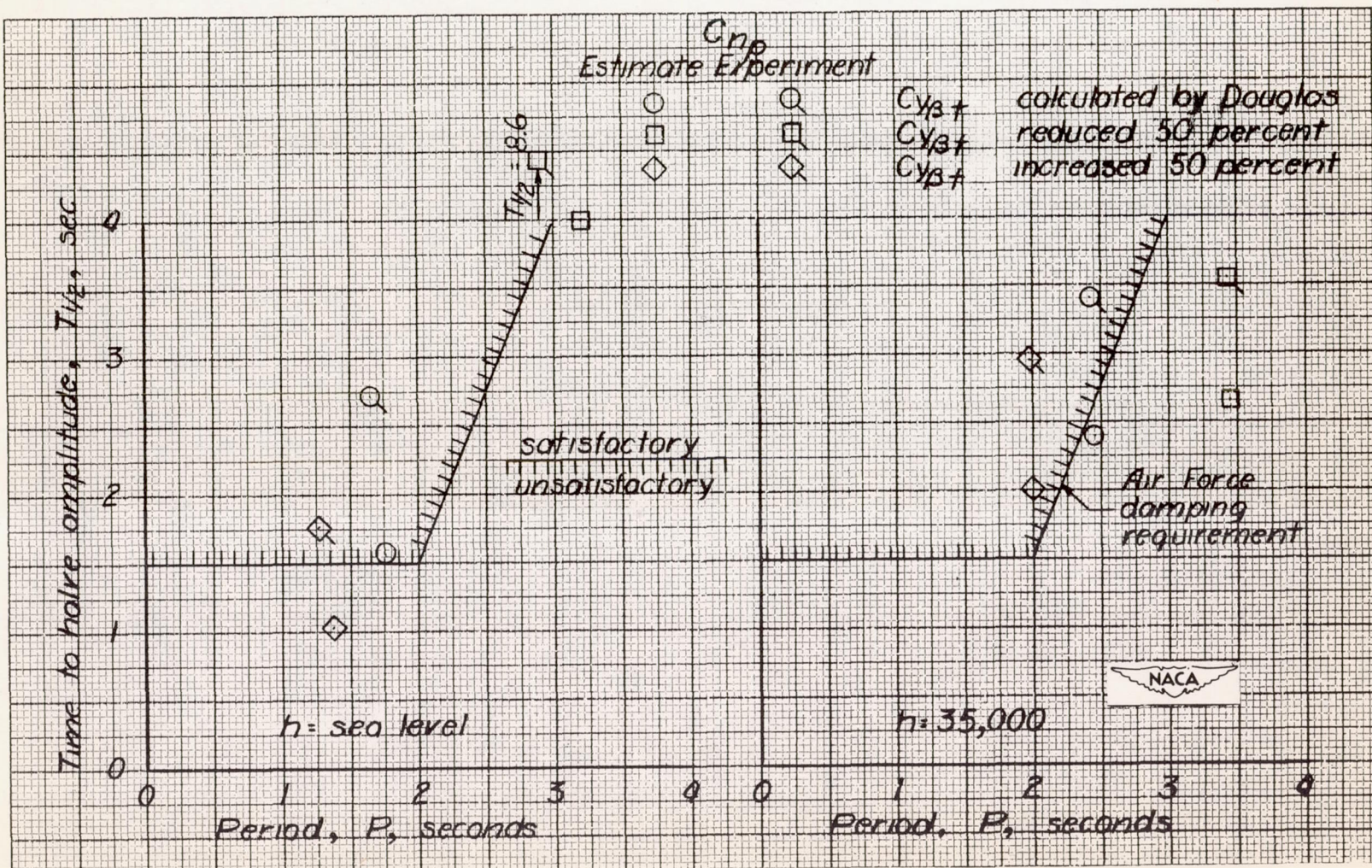


Figure 2.- Effect on the period and damping of increasing or decreasing  $C_{Y\beta_t}$  by 50 percent for values of  $C_{np}$  that were estimated and for those that were based on experiment.  $M = 0.75$ .

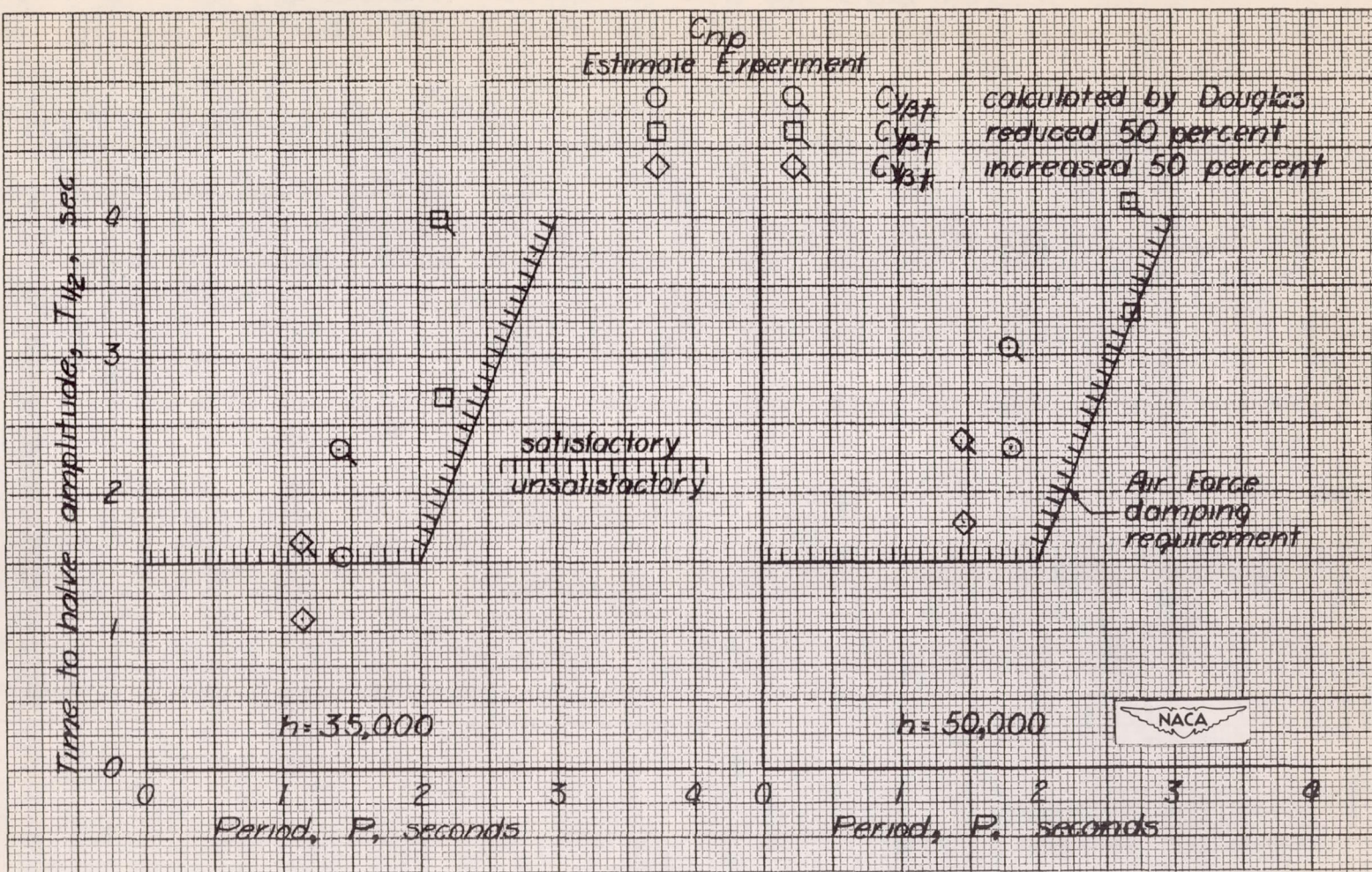


Figure 3.- Effect on the period and damping of increasing or decreasing  $C_{y\beta_t}$  by 50 percent for values of  $C_{n_p}$  that were estimated and for those that were based on experiment.  $M = 1.2$ .

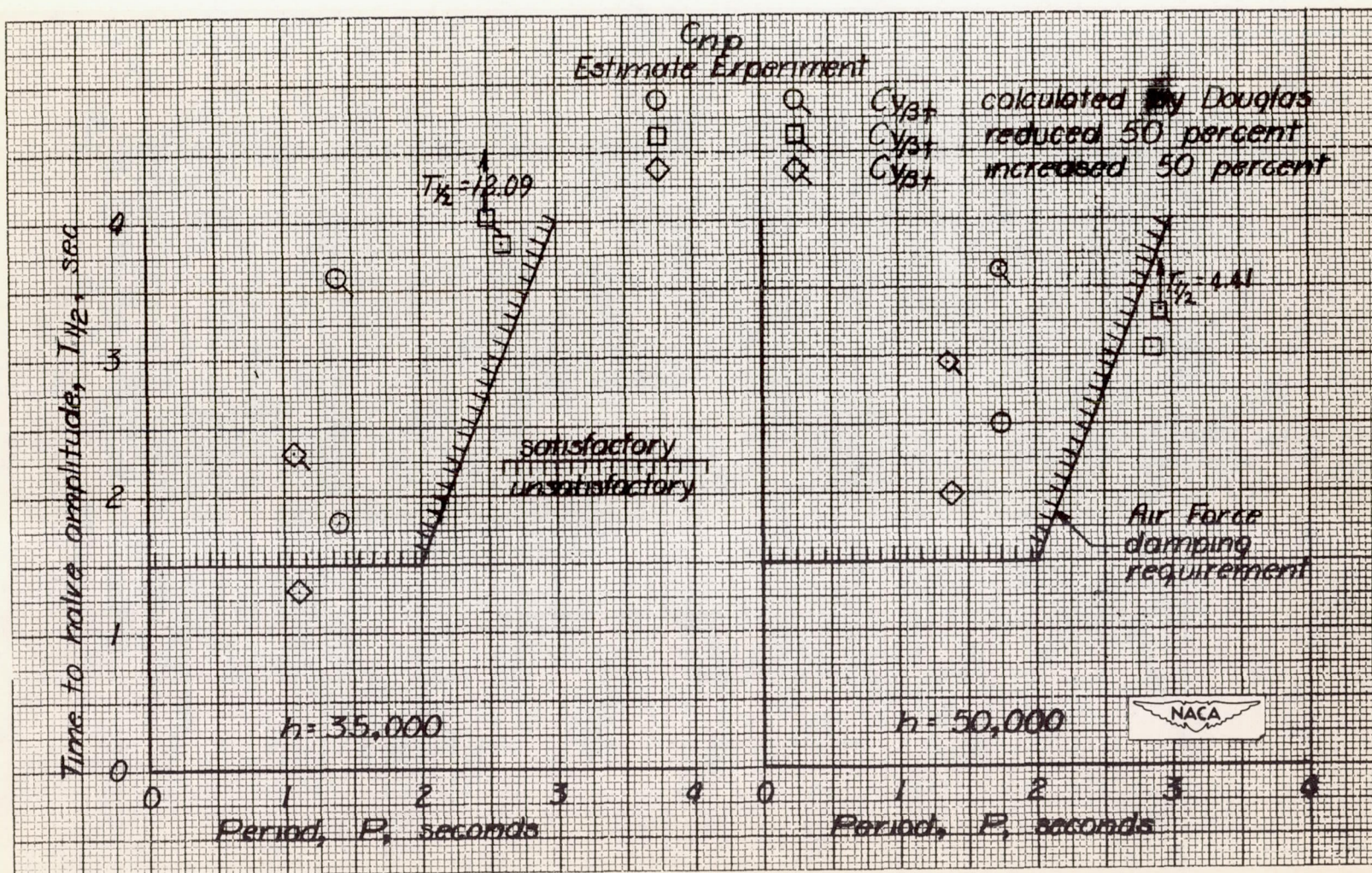


Figure 4.- Effect on the period and damping of increasing or decreasing  $C_{y\beta}$  by 50 percent for values of  $C_{n_p}$  that were estimated and for those that were based on experiment.  $M = 2.0$ .

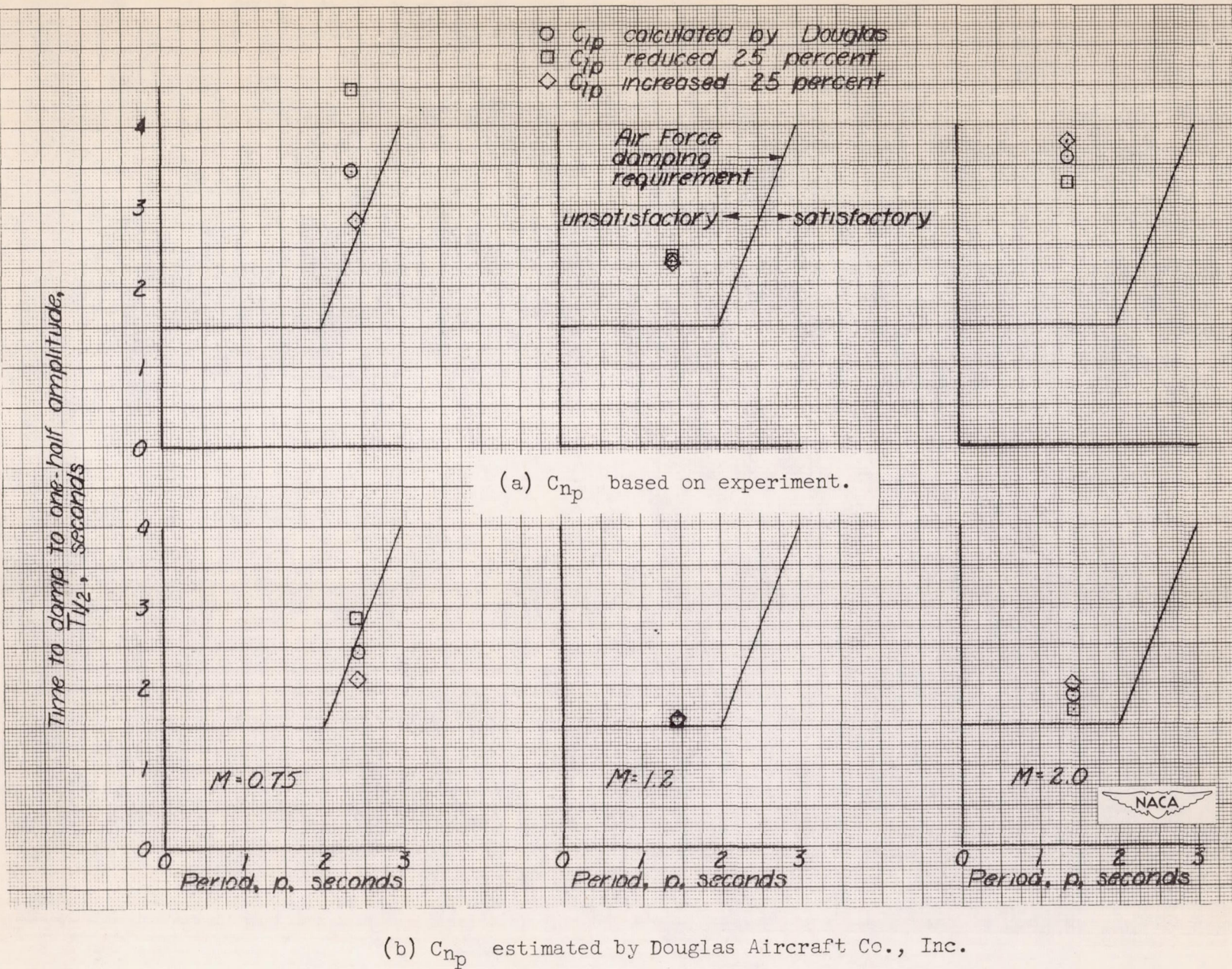


Figure 5.- Effect on the period and time to damp of increasing or decreasing  $C_{l_p}$ .  $h = 35,000$  feet.

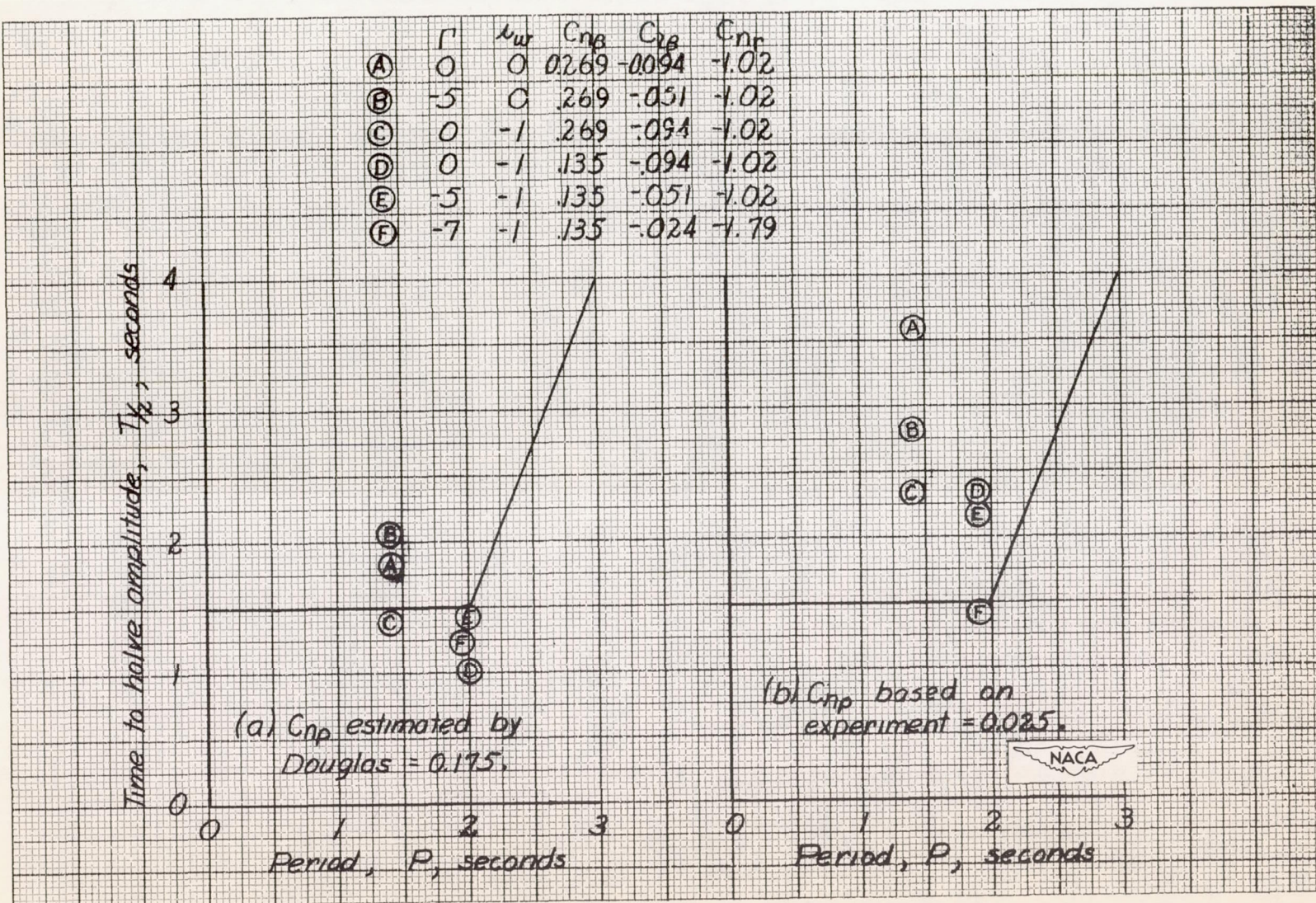


Figure 6.- Effect on the period and time to damp to one-half amplitude of several geometric changes to the Douglas X-3 airplane.  $M = 2.0$ .  $h = 35,000$  feet.

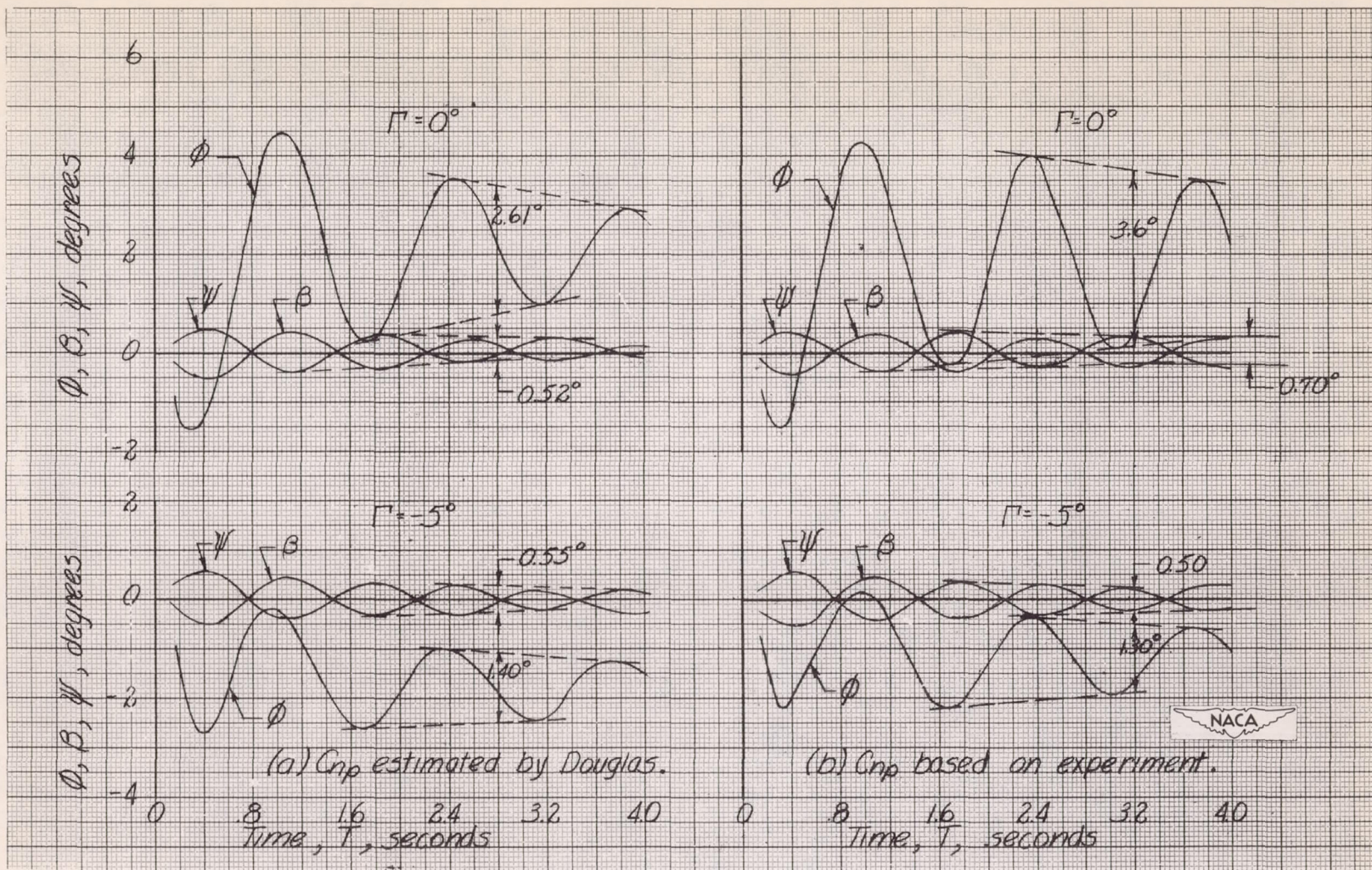


Figure 7.- Effect on the calculated motion of a 0.15 second rudder kick of  $C_n = 0.004$  and  $C_l = 0.001$  (approx.  $2.5^\circ$  rudder deflection) for geometric dihedral angles of  $0^\circ$  and  $-5^\circ$ .

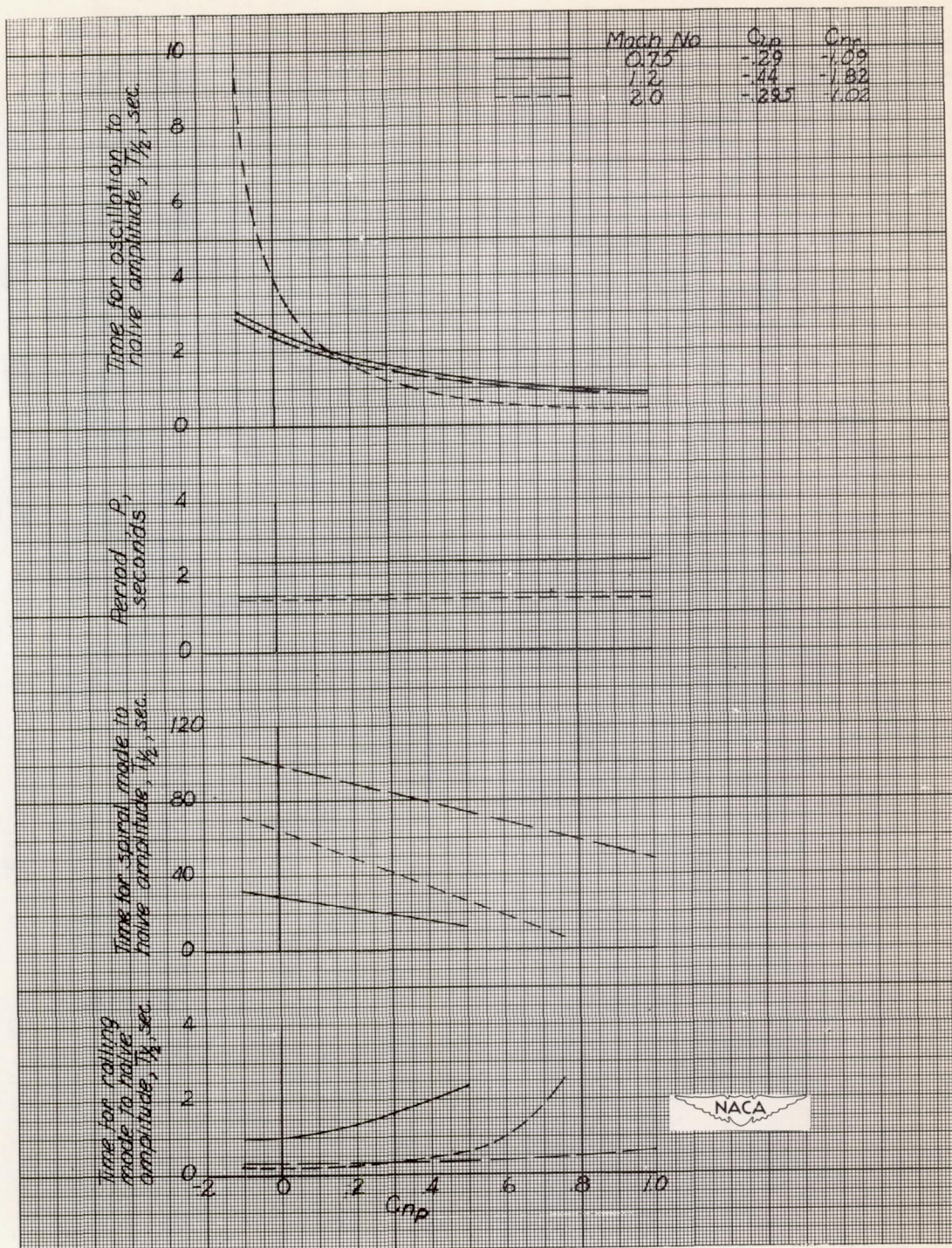


Figure 8.- Effect on the period and damping of varying  $C_{n_p}$  to simulate the addition of a rate gyro autopilot with zero time lag.  
 $h = 35,000$  feet.

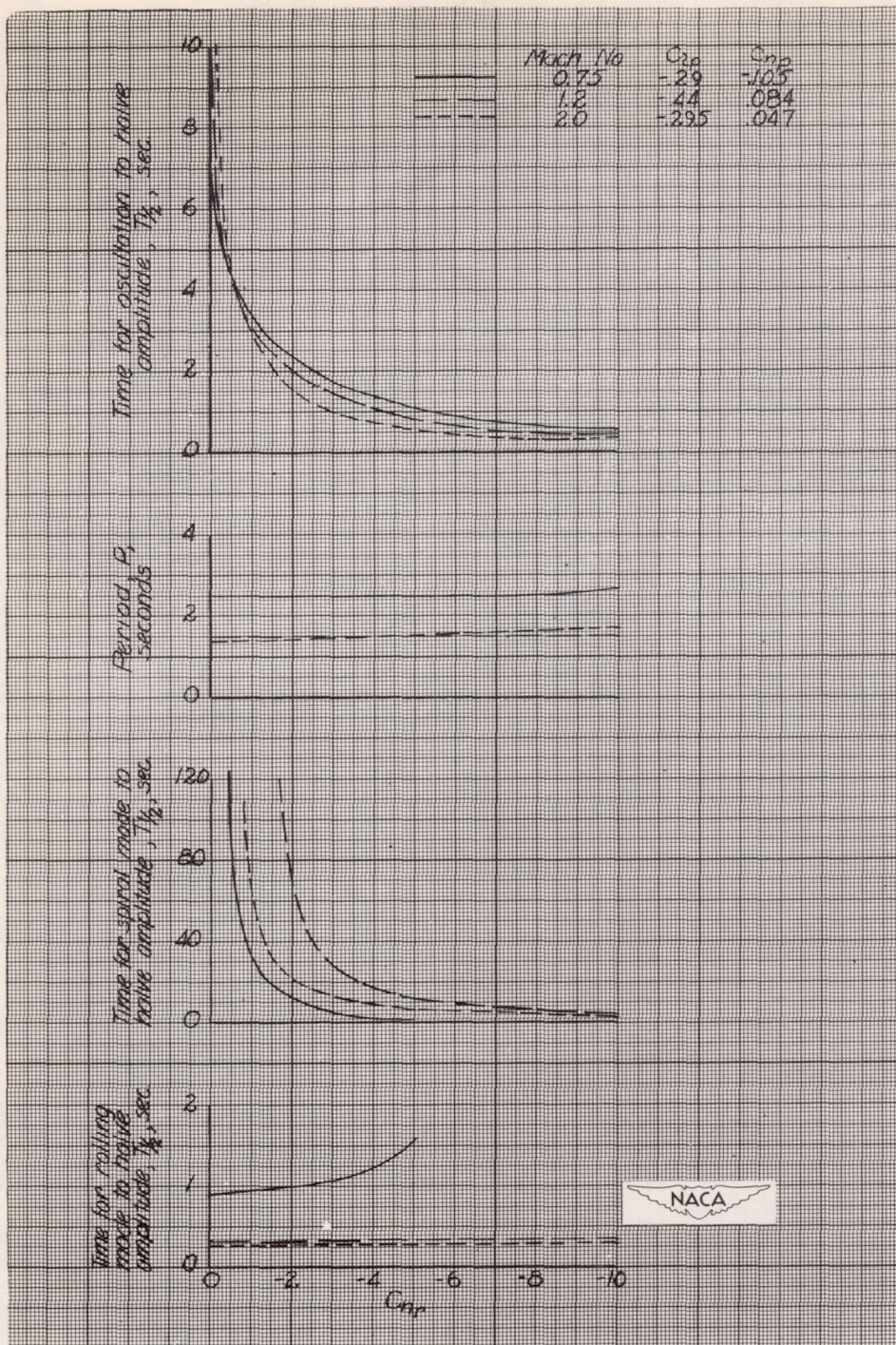


Figure 9.- Effect on the period and damping of varying  $C_{n_r}$  to simulate the addition of a rate gyro autopilot with zero time lag.  
 $h = 35,000$  feet.

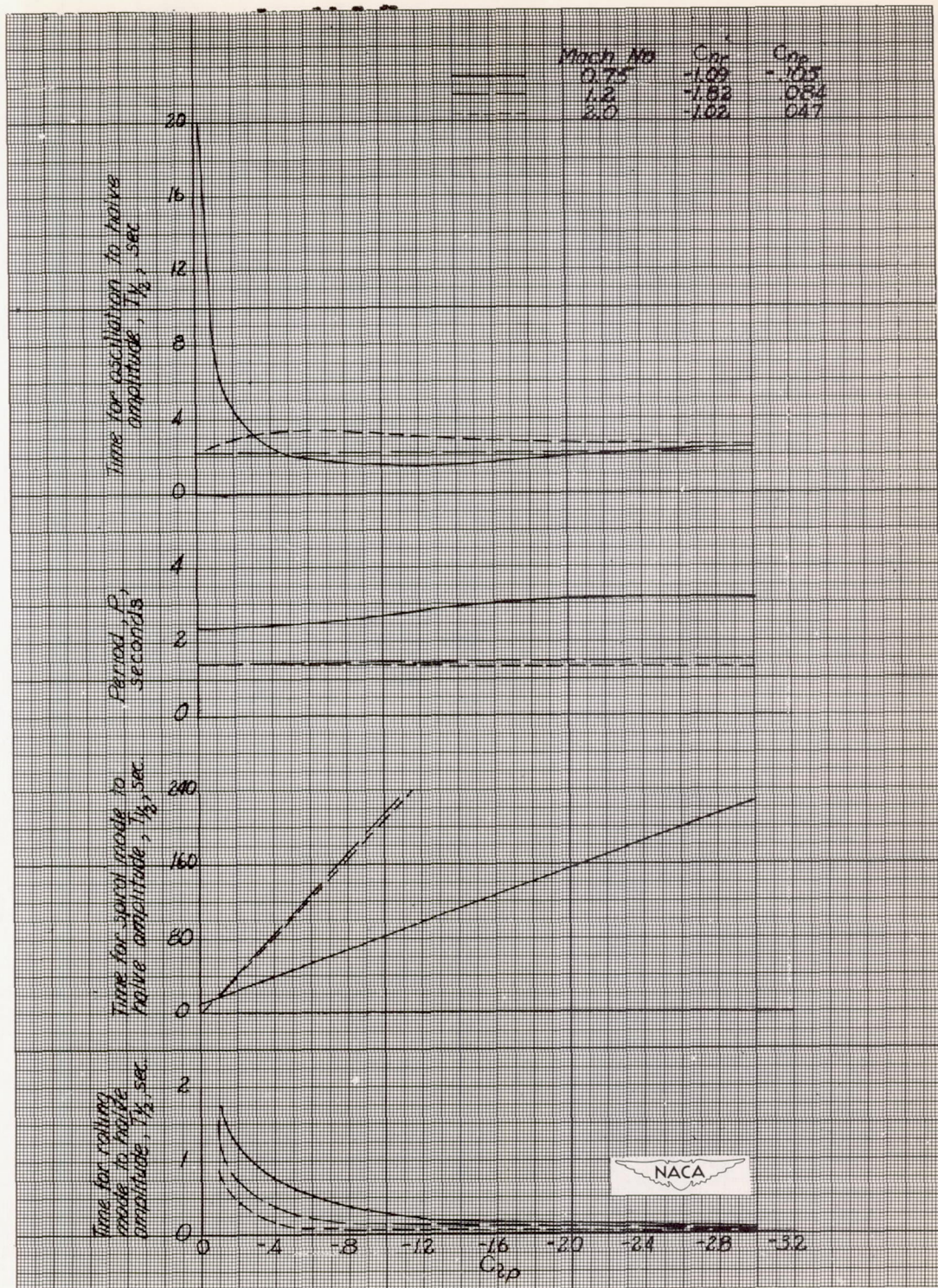


Figure 10.- Effect on the period and damping of varying  $C_{l_p}$  to simulate the addition of a rate gyro autopilot with zero time lag.  
 $h = 35,000$  feet.

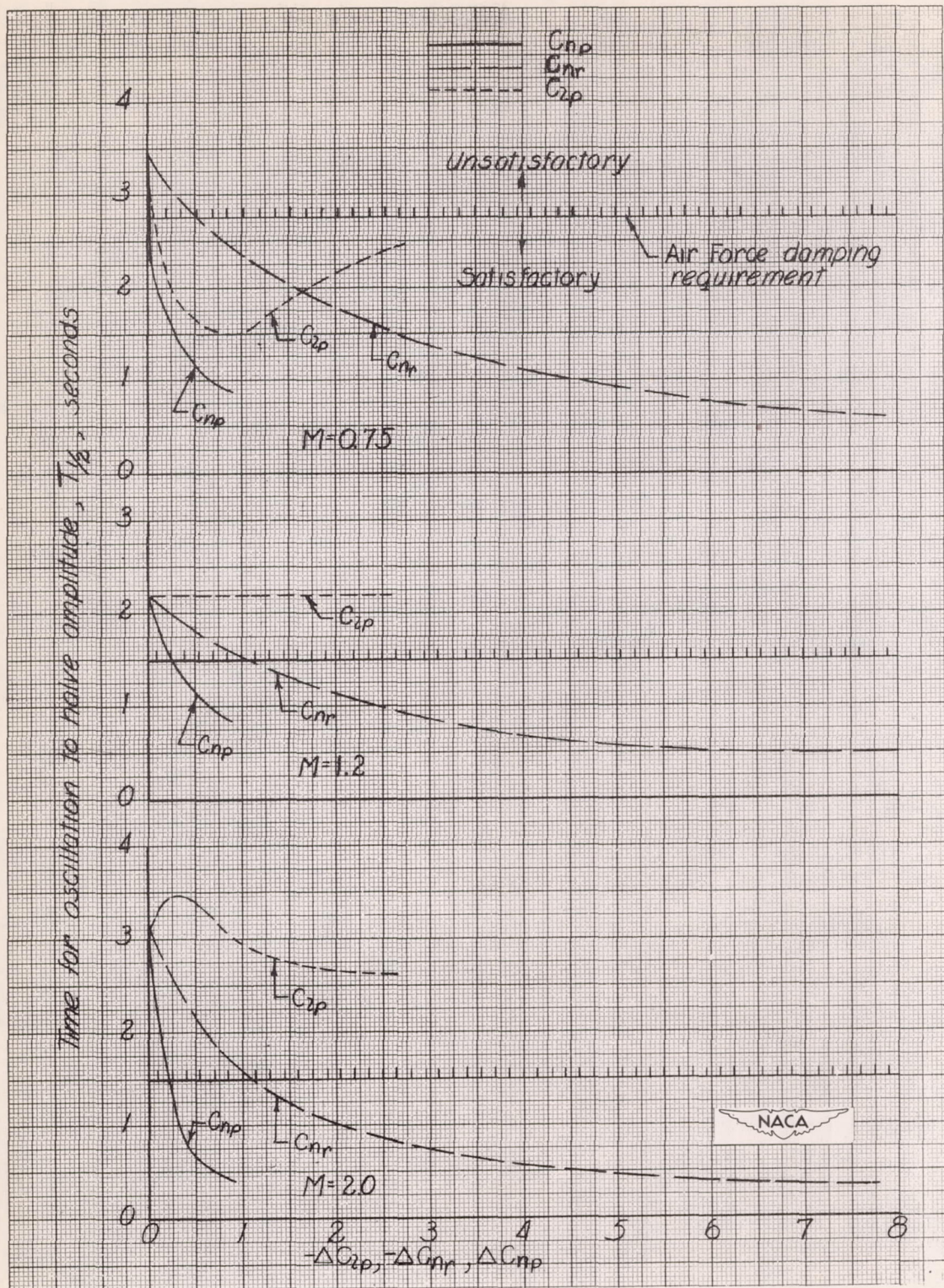


Figure 11.- A comparison of the effects on the damping of the lateral oscillation of adding three types of autopilot.  $h = 35,000$  feet.

